

# DNA Microarray Analysis of Hypothermic Murine Myocardium to Study Pathophysiology and Identify Forensic Biomarkers

**Keywords:** Heart; Myocardium; Hypothermia; Transcriptome; DNA microarray; Quantitative PCR

## Abstract

We used DNA microarray technology to analyze the myocardial transcriptome of mice killed via experimentally induced hypothermia. This analysis identified significant differential regulation of 3438 genes; specifically, 1704 genes were upregulated, and 1734 were downregulated in response to hypothermia. The gene encoding granzyme A was the most upregulated gene, and that encoding solute carrier family 41 member 3 was the most downregulated. Gene-set analysis identified significant hypothermia-induced variation in 79 pathways, and we suggest that pathways related to granzyme A and cell death may be involved in cardiac pathogenesis of hypothermia. Gene-function-category analysis demonstrated the most highly represented categories among the upregulated and downregulated genes were cellular process (biological process), binding (molecular function), and cell and cell part (cellular component). The presented findings clearly demonstrated that acute myocardial responses to hypothermia did occur; they also indicated several cardiac-related candidate genes as forensic biomarkers of hypothermia. Hypothermia-induced myocardial cell death would be an irreversible change that, we believe, may explain the circulatory failure, resistance to treatment, and high mortality associated with hypothermia. Furthermore, the present microarray data may facilitate development of immunohistochemical analysis and protocols to be used for human forensics and may be beneficial in clinical research on hypothermia.

## Introduction

Hypothermia is classically defined as a core body temperature of less than 35 °C. Hypothermia develops when adaptive thermoregulatory mechanisms are overwhelmed and hypothermia is a common danger even indoors and in temperate climates [1,2]. Macroscopically, hypothermia may cause the following: frostbite; bright-pink lividity [3]; hemorrhages in muscles [4]; cerebral edema [3]; venous thrombosis [2]; pulmonary edema [2,3,5]; bronchopneumonia [6]; hemorrhages in the stomach, ileum, and colon [3,5,6]; and diuresis [5]. Additionally, histological examinations reveal fatty changes in the liver and kidneys [7-9], vacuolization of liver cells [3] and pancreatic adenoid cells [10], renal tubular necrosis [5,6], heat shock protein 70 accumulation in renal tubular epithelium and glomerular podocytes [11], and hemorrhagic pancreatitis [3,5,6,8]. Forensic differential diagnosis of hypothermia is often difficult because many of these autopsy findings are not specific to hypothermia. Therefore, diagnosis of hypothermia must be based partly on exclusion criteria and historical information. However, molecular biological methods may provide more definitive criteria for forensic diagnosis of hypothermia [12].

Hypothermia carries a high mortality rate due to circulatory



## Journal of Forensic Investigation

Masataka Takamiya<sup>1\*</sup>, Kiyoshi Saigusa<sup>2</sup> and Koji Dewa<sup>1</sup>

<sup>1</sup>Department of Forensic Medicine, Iwate Medical University, Iwate, Japan

<sup>2</sup>Department of Biology, Iwate Medical University, Iwate, Japan

### \*Address for Correspondence

Masataka Takamiya MD, PhD, Department of Forensic Medicine, Iwate Medical University, 2-1-1 Nishitokuta, Yahaba, Iwate 028-3694, Japan, Tel: +81-19-698-1820; Fax: +81-19-908-8005; E-mail: mtakamiy@iwate-med.ac.jp

**Submission:** 20 January, 2016

**Accepted:** 16 March, 2016

**Published:** 21 March, 2016

**Copyright:** © 2016 Takamiya M, et al. This is an open access article distributed under the Creative Commons Attribution License, which permits unrestricted use, distribution, and reproduction in any medium, provided the original work is properly cited.

**Reviewed & Approved by:** Dr. Robert Allen, Oklahoma State University, Center for Health Sciences, USA

failure [13]. Cardiac output and sinus rate decrease and arrhythmias (from atrial fibrillation to ventricular fibrillation) occur during hypothermia [14,15]. Therefore, it is important to document the cardiovascular state during hypothermia; consequently, we considered it worthwhile to assess hypothermia-induced changes to the myocardial transcriptome. In this study, the myocardial transcriptome in hypothermic mice was analyzed to examine the cardiac pathophysiology of mammalian hypothermia and to identify candidates for forensic biomarkers of human hypothermia. This study was designed both for the study of cardiac pathophysiology and to improve forensic practices; moreover, the findings should be beneficial for clinical research on hypothermia.

## Materials and Methods

### Tissue samples

A water-bath method described previously was adapted to induce hypothermia in mice [16]. Male ddY mice 7 weeks of age and weighing  $36.3 \pm 6.8$  g were housed under controlled lighting (lights on at 7:00 am and off at 7:00 pm) and given free access to food and water. This was a preliminary study, and only male mice were used; therefore, potential differences due to sex should be addressed in future studies. Each mouse was anesthetized by sevoflurane inhalation and then confined in a metallic restraint cage that was kept in a water bath set at 10 °C such that each mouse was immersed up to the neck in the cold water. Each animal died from continuous exposure to cold water for  $42.8 \pm 12.6$  minutes. Immediately after death, a 2-mm thick specimen from the anterior wall of the left ventricle was resected 3 mm from the heart apex for each animal. In all, 28 mice were subjected to hypothermia-induced death; four were used for DNA microarray analyses, four for selection of genes to be used as the internal standard, 10 for quantitative PCR analyses, and 10 for immunohistochemical

analyses. Control mice (n = 28) were sacrificed by inhalation of CO<sub>2</sub>, and the same part of each control left ventricle was examined (n = 4 for DNA microarray, n = 4 for internal standard gene selection, n = 10 for quantitative PCR, n = 10 for immunohistochemistry). Because this was a forensic pathologic study, samples from hypothermic and separately control mice were collected from cadavers. In other words, death was the most important commonality between the hypothermic and control mice. Furthermore, the interval between initial CO<sub>2</sub> exposure and death was extremely short in the control group, and this short time period may have precluded substantial changes in gene expression; therefore, CO<sub>2</sub> exposure was an appropriate negative-control treatment for our purposes. For DNA microarray analyses, internal standard gene selection, and quantitative PCR analyses, each isolated tissue specimen was immediately soaked in 1.5 ml RNAlater solution (Applied Biosystems, Carlsbad, CA), and stored at -80 °C for 2 weeks. The research described in this report was conducted in accordance with the guidelines for animal experimentation from Iwate Medical University.

### DNA microarray methods

RNeasy Fibrous Tissue Mini Kits (Qiagen, Valencia, CA) were used to extract total RNA samples from tissue specimens. All microarray procedures described here were performed at Tohoku Chemical Research Institute of Bio-system Informatics (Morioka, Japan). Electrophoresis through a 1% agarose gel, an absorptiometer, and a 2100 bioanalyzer (Agilent Technologies, Santa Clara, CA) were used to confirm the quality of the RNA samples; quality control criteria were as follows: OD260/280 > 1.5, OD260/230 > 1.0, no degradation in electrophoresis, 28S/18S ribosomal RNA bands > 1.8, RNA Integrity Number > 7. The Mouse GE 4x44K v2 Microarray Kit (4 arrays, Agilent Technologies, Santa Clara, CA) was used according to the manufacturer's instructions to determine gene expression profiles. The analysis was performed with the two-color method; control samples were labeled with Cy3, and hypothermic samples were labeled with Cy5. Scanning of microarray slides was performed with Agilent Technologies Scanner G2505C and Agilent Feature Extraction 10.7.3.1 (Agilent Technologies, Santa Clara, CA). For further analysis, GeneSpring (Agilent Technologies, Santa Clara, CA) was also used. In addition, annotations of genes were based on the Gene and GenBank of National Center for Biotechnology Information (NCBI, Bethesda, MD). Thus, those probes that are not cataloged in Gene or GenBank were not annotated in the present study. This experiment was verified according to the minimum information about microarray experiment (MIAME) guidelines (Supplement 1) [17].

**Quality control:** Quality control for each feature (spot) was performed using the settings recommended by Agilent Technologies. Background signal was subtracted, and signal intensity of each feature was globally normalized via locally weighted scatter-plot smoothing (LOWESS). The following flag parameters were used: "Feature is saturated"; "Feature is not uniform"; "Feature is not positive and significant"; "Feature is not above background"; "Feature is a population outlier". For each of these parameters, one of the following terms was applied to each feature:

Detected: The data are reliable.

Not detected: The quality of data are undetermined.

Compromised: The data are unreliable.

Each gene was represented by four spots, and one of the following terms was applied to each spot:

Detected: All the parameters are "Detected".

Not detected: The parameters are combinations of "Detected" and "Not detected".

Compromised: One of the parameters is "Compromised".

For subsequent analyses, we used only genes for which all four spots were categorized as "Detected".

**Selection of significantly regulated genes:** The one-sample Student's t-test was performed to identify genes that exhibited significant differential expression in response to hypothermia. P values of 0.05 or lower were considered statistically significant. After the correction for multiple tests (Benjamini-Hochberg method), only five genes showed significant differences between the experimental and control samples. This phenomenon was due to the dispersion of gene expression data among four arrays. Therefore, these statistical methods were not used.

### Gene-set analysis:

**KEGG analysis:** We used the KEGG (Kyoto Encyclopedia of Genes and Genomes) pathway database and previously published methods to perform gene-set analysis [18]. The mean of fold-changes among all quality-controlled genes were compared to the fold-change of each gene set. Z scores of fold-changes were calculated, and datasets with normal distributions were subject to statistical analysis. P values of 0.05 or lower were considered statistically significant.

**Analyses with publically available pathway databases:** Biocarta pathway (San Diego, CA) and GeneAssist (Applied Biosystems, Waltham, MA) are publically available pathway databases. In addition to KEGG, supplementary analyses of gene sets were performed with each of these databases. For pathway selection, three upregulated genes (granzyme A: *Gzma*; cytochrome P450, family 26, subfamily b, polypeptide 1: *Cyp26b1*; and activating transcription factor 3: *Atf3*) and three downregulated genes (solute carrier family 41, member 3: *Slc41a3*; solute carrier family 46, member 2: *Slc46a2*; and nuclear receptor subfamily 1, group D, member 1: *Nr1d1*) were used.

**Analysis with Biocarta pathway:** Biocarta pathway (San Diego, CA) is an open-source database; the information is displayed in a graphical format, and known genomic and proteomic relationships are mapped. In connection with the six selected genes, a granzyme A-mediated apoptosis pathway was retrieved for *Gzma*. Using previously published methods, a gene-set analysis was performed with this pathway [18].

**Analysis with GeneAssist:** More than 350 different pathways are currently available in GeneAssist (Applied Biosystems, Waltham, MA). Illustrations show molecular interactions and cellular compartments. In connection with the six selected genes, the following five pathways were found in this database: the granzyme, granzyme A, IL 9 pathways (for *Gzma*), and the MAPK signaling

**Table 1:** Genes upregulated by hypothermia in myocardium arranged in descending order based on fold-change.

Probe name	Fold change	Description	Symbol	RefSeq
A_55_P1960148	3.310967386			
A_55_P2094060	3.258506336	granzyme A	Gzma	NM_010370
A_51_P509679	3.207406257			
A_51_P501844	2.523991759	cytochrome P450, family 26, subfamily b, polypeptide 1	Cyp26b1	NM_001177713, NM_175475
A_52_P452689	2.401837922	activating transcription factor 3	Atf3	NM_007498
A_55_P2220937	2.213662067	OTU domain containing 1	Otud1	NM_027715
A_51_P153486	2.062825093	DnaJ (Hsp40) homolog, subfamily B, member 1	Dnajb1	NM_018808
A_55_P2024155	2.02340035	zinc finger and BTB domain containing 16	Zbtb16	NM_001033324
A_55_P2185330	1.994610652	predicted gene 10914	Gm10914	XR_141300, XR_141788
A_55_P2087984	1.978908627	DnaJ (Hsp40) homolog, subfamily A, member 1	Dnaja1	NM_001164671, NM_001164672, NM_008298
A_55_P2060897	1.972709744	immunoglobulin kappa constant	Igkc	
A_55_P1993404	1.95759763			
A_55_P2098120	1.951765504	EMI domain containing 2	Emid2	NM_024474
A_51_P511250	1.929251998	family with sequence similarity 46, member B	Fam46b	NM_175307
A_55_P1990314	1.917089432	ELAV (embryonic lethal, abnormal vision, Drosophila)-like 4 (Hu antigen D)	Elavl4	NM_001038698, NM_001163397, NM_001163399, NM_010488
A_55_P2165869	1.904172132	CCAAT/enhancer binding protein (C/EBP), beta	Cebpb	NM_009883
A_51_P113178	1.88886637	RIKEN cDNA 6530418L21 gene	6530418-L21Rik	NM_001163356, NM_175398
A_55_P2040026	1.881154835	integrin alpha 4	Itga4	NM_010576
A_55_P2073612	1.849744873	fibroblast growth factor 6	Fgf6	NM_010204
A_55_P2064741	1.832918197	neuromedin B	Nmb	NM_026523
A_55_P2021109	1.821057972	immediate early response 5	Ier5	NM_010500
A_55_P2103452	1.809820605	neuropeptide Y receptor Y1	Npy1r	NM_010934
A_55_P1954271	1.80959085	EMI domain containing 2	Emid2	NM_024474
A_55_P2033665	1.791293364			
A_55_P2135967	1.786622703			
A_55_P1980521	1.776449775	coiled-coil domain containing 85A	Ccdc85a	NM_181577, NM_001166661, NM_001166662
A_55_P2014506	1.764043577	S-adenosylmethionine decarboxylase 2	Amd2	NM_007444
A_55_P2095118	1.761115416	RIKEN cDNA 2700023E23 gene	2700023-E23Rik	NR_015531
A_51_P406557	1.743799778	expressed sequence AI464131	AI464131	NM_001085515
A_55_P2173073	1.72924322	zinc finger protein 931	Zfp931	NM_001162922
A_66_P102090	1.700395481	protein kinase, membrane associated tyrosine/threonine 1	Pkmyt1	NM_023058
A_52_P38639	1.691520545	fermitin family homolog 3 (Drosophila)	Fermt3	NM_153795
A_55_P2126269	1.690532158	neuromedin B	Nmb	NM_026523
A_55_P2000521	1.68909796	LON peptidase N-terminal domain and ring finger 1	Lonrf1	NM_001081150
A_55_P2279807	1.689042278	RIKEN cDNA 6720427I07 gene	6720427-I07Rik	
A_55_P2172274	1.679279997	structural maintenance of chromosomes 2	Smc2	NM_008017
A_55_P1997225	1.64774735	ArfGAP with GTPase domain, ankyrin repeat and PH domain 2	Agap2	NM_001033263
A_55_P2344608	1.638536374	DNA segment, Chr 7, Wayne State University 130, expressed	D7Wsu130e	
A_55_P1967133	1.638386235	protein phosphatase 1, regulatory (inhibitor) subunit 3B	Ppp1r3b	NM_177741

A_55_P1974347	1.634805044	family with sequence similarity 126, member B	Fam126b	NM_172513
A_55_P2161675	1.632035965	zinc finger protein 133, pseudogene	Zfp133-ps	NR_033459
A_55_P2014511	1.623175349	S-adenosylmethionine decarboxylase 2	Amd2	NM_007444
A_55_P2087985	1.621794809			
A_55_P1991778	1.620374684	RIKEN cDNA 2310028H24 gene	2310028-H24Rik	NM_001159583, NM_027993
A_55_P1997300	1.619203036	family with sequence similarity 54, member A	Fam54a	NM_027930
A_55_P2011727	1.613928091	neuralized homolog 1b (Drosophila)	Neurl1b	NM_001081656
A_55_P2031436	1.613402504	lymphocyte antigen 6 complex, locus E	Ly6e	NM_001164039, NM_001164040, NM_008529, NM_001164036, NM_001164037, NM_001164038
A_55_P2034864	1.608376375	tubulin, beta 2B class IIB	Tubb2b	NM_023716
A_51_P212741	1.603121499	sodium channel, voltage-gated, type II, beta	Scn2b	NM_001014761
A_55_P2045682	1.60071475	Ras association (RalGDS/AF-6) domain family member 5	Rassf5	NM_018750

**Table 2:** Genes downregulated by hypothermia in myocardium arranged in ascending order based on fold-change.

Probe name	Fold change	Description	Symbol	RefSeq
A_55_P2041286	0.377100195	predicted gene 3970	Gm3970	XM_001479374, XM_001479641
A_51_P442097	0.462881497	solute carrier family 41, member 3	Slc41a3	NM_001037493, NM_027868
A_55_P2219731	0.464501513	expressed sequence AI413759	AI413759	
A_55_P2021187	0.478583545	metastasis associated lung adenocarcinoma transcript 1 (non-coding RNA)	Malat1	NR_002847
A_51_P185763	0.478656498	solute carrier family 46, member 2	Slc46a2	NM_021053
A_55_P1975425	0.487999069	RIKEN cDNA 2210417A02 gene	2210417-A02Rik	NR_028285
A_51_P223776	0.493093691	nuclear receptor subfamily 1, group D, member 1	Nr1d1	NM_145434
A_55_P1991693	0.49658256	peroxisome proliferative activated receptor, gamma, coactivator-related 1	Pprc1	NM_001081214, NM_145504
A_55_P1986711	0.502051616			
A_55_P2185185	0.515100662	transmembrane protein 28	Tmem28	NM_001081283
A_52_P337232	0.528463487	RIKEN cDNA B230340J04 gene	B230340-J04Rik	NM_177234
A_55_P2053923	0.534205006	RAB17, member RAS oncogene family	Rab17	NM_008998, NM_001159725
A_55_P1985638	0.535924115	shisa homolog 7 (Xenopus laevis)	Shisa7	NM_172737
A_55_P2201020	0.541205985	expressed sequence AI790442	AI790442	
A_66_P120770	0.5438703	tyrosine 3-monooxygenase/tryptophan 5-monooxygenase activation protein, zeta polypeptide	Ywhaz	NM_001253805, NM_001253806, NM_001253807, NM_011740
A_55_P2018836	0.546349483			
A_55_P2049687	0.546643661	ephrin A2	Efna2	NM_007909
A_55_P2063937	0.548479194			
A_55_P2180744	0.551811504	calsyntenin 3	Clstn3	NM_153508
A_55_P2107247	0.561537303	testis-specific serine kinase 5	Tssk5	NM_183099
A_55_P2136533	0.561899659	myeloid/lymphoid or mixed-lineage leukemia 2	Mll2	NM_001033388, NM_001033276
A_51_P436491	0.565783198	leucine rich repeat and Ig domain containing 3	Lingo3	NM_001013758
A_55_P2036813	0.570474221	histone cluster 3, H2ba	Hist3h2ba	NM_030082
A_55_P2121613	0.576058902	SRY-box containing gene 4	Sox4	NM_009238
A_51_P240253	0.585840952	Ras-related associated with diabetes	Rrad	NM_019662
A_51_P415395	0.586204359	C2 calcium-dependent domain containing 4B	C2cd4b	NM_001081314
A_55_P2025483	0.588201839	Rieske (Fe-S) domain containing	Rfesd	NM_001131068, NM_001131069, NM_178916

A_55_P2119927	0.589530762			
A_55_P2010539	0.589885397			
A_55_P2007776	0.598626935	cation channel, sperm associated 2	Catsper2	NM_153075

and TNF signaling pathways (for *Atf3*). Using previously published methods, gene-set analyses were performed with these pathways [18].

**Gene functional-category analysis:** Gene functional-category analyses were performed. The number of genes corresponding to each Gene Ontology term among all genes was compared to the number among differentially regulated genes using Fisher’s Exact Test. P values of 0.05 or lower was considered statistically significant.

**Quantitative PCR**

To validate selected aspects of microarray results, three upregulated genes (*Gzma*, *Cyp26b1*, *Atf3*; Table 1) and three downregulated genes (*Slc41a3*, *Slc46a2*, *Nr1d1*; Table 2) were selected for measurement by quantitative PCR.

**RNA extraction and reverse transcription:** Total RNA was extracted from tissues using an RNeasy Fibrous Tissue Mini Kit (Qiagen, Valencia, CA). An absorptiometer and electrophoresis through a 1% agarose gel were used to confirm the quality of the RNA samples; the quality control criteria were as follows: OD260/280 > 1.5, OD260/230 > 1.0, no degradation in electrophoresis with 28S and 18S ribosomal RNA bands. The RNA was treated with TURBO DNase (Applied Biosystems, Waltham, MA). A High-Capacity cDNA Reverse Transcription kit with RNase inhibitor (Applied Biosystems, Waltham, MA) was then used according to the manufacturer’s instructions to synthesize cDNA.

**Real-time quantitative PCR:** TaqMan Gene Expression Assays (Applied Biosystems, Waltham, MA) are the most reliable sets of pre-

designed quantitative real-time PCR assays. TaqMan Gene Expression Assays (Applied Biosystems, Waltham, MA) have been designed using the validated bioinformatics pipeline and run with the same PCR protocol; this protocol eliminates the need for time-consuming primer design or PCR optimization. TaqMan Gene Expression Assays (Applied Biosystems, Waltham, MA) are used as the gold standard technology in mRNA quantification. In the present study, TaqMan Gene Expression Assays (Applied Biosystems, Waltham, MA) were used with the following primers and probes:

- Gzma*: Mm01304452\_m1, NM\_010370.2, 59bp
- Cyp26b1*: Mm00558507\_m1, NM\_001177713.1, NM\_175475.3, 75bp
- Atf3*: Mm00476032\_m1, NM\_007498.3, 61bp
- Slc41a3*: Mm01182529\_m1, NM\_001037493.2, NM\_027868.2, 91bp
- Slc46a2*: Mm00498614\_m1, NM\_021053.4, 64bp
- Nr1d1*: Mm00520708\_m1, NM\_145434.4, 62bp

A value that represents the stability of individual internal-standard genes was used to select the internal-standard gene; values for β-actin, glyceraldehyde-3-phosphate dehydrogenase (*GAPDH*), and 18S ribosomal RNA were 1.68, 1.52 and 1.96 respectively [19]. Therefore, *GAPDH* was used as the internal-standard gene. *GAPDH* primers and probes are supplied with TaqMan Gene Expression Assays (Mm9999915\_g1, NM\_001289726.1, NM\_008084.3, 107bp,

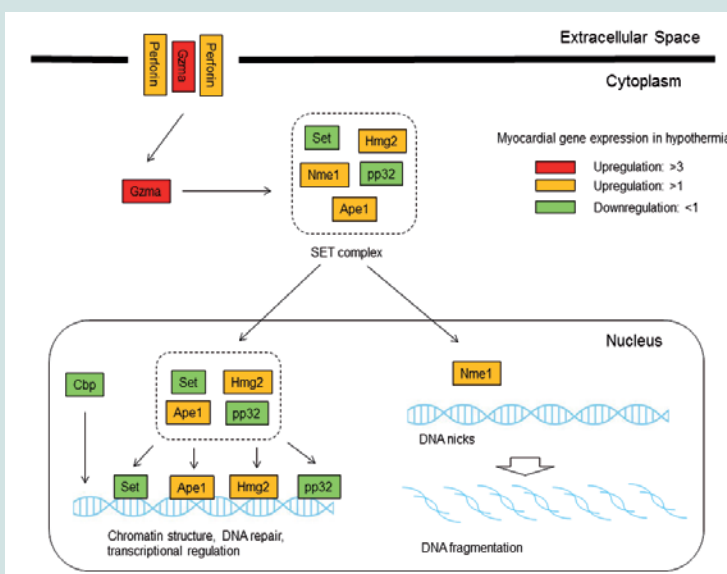


**Figure 1:** Hypothermia-induced granzyme A-mediated apoptosis pathway. Granzyme A causes DNA fragmentation. The pathway shown was constructed based on information from the Biocarta pathway database (San Diego, CA). Gene names are as follows: *Ape1*: apurinic/apyrimidinic endonuclease 1; *Cbp*: CREB binding protein; *Gzma*: granzyme A; *Hmg2*: high-mobility group protein B2; *Nme1*: NME/NM23 nucleoside diphosphate kinase 1; *pp32*: acidic (leucine-rich) nuclear phosphoprotein 32 family, member A; *Set*: SET nuclear oncogene.

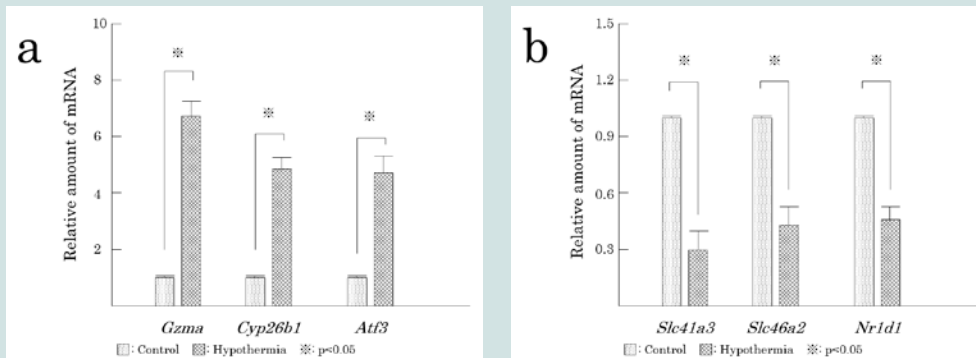


**Figure 2:** Real-time quantitative PCR analysis of six representative genes, three upregulated (a) and three downregulated (b). Hypothermia-associated mRNA levels relative to control levels. Values are each a mean ± SD (n = 10 for hypothermic mice, n = 10 for control mice).

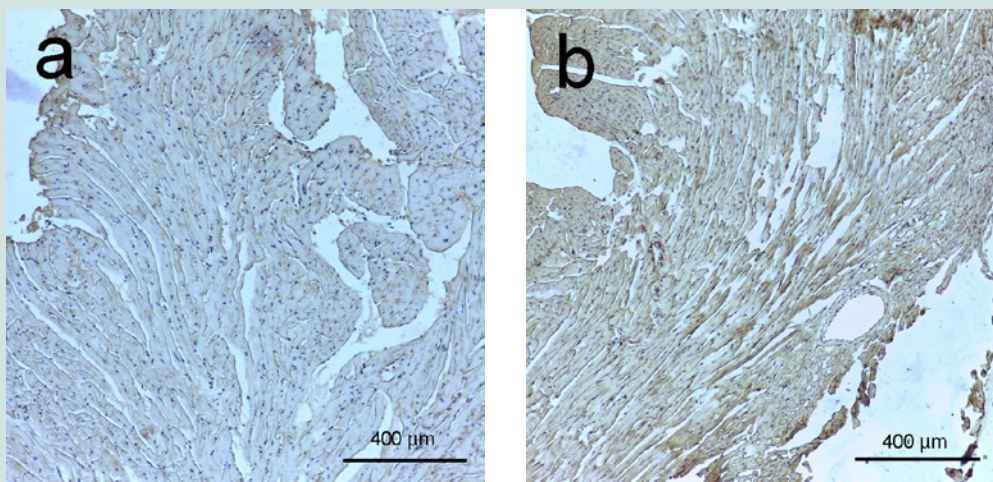


**Figure 3:** Immunohistochemistry of Granzyme A. Granzyme A signal was not evident in control specimens from left ventricle tissue (a). Cardiac myocytes showed some cytoplasmic expression of granzyme A in specimens from each hypothermic left ventricle (b). Granzyme A expression was not evident in any endocardial, epicardial, or endothelial cells.

Applied Biosystems, Waltham, MA). Real-time quantitative PCR was performed using a PRISM 7500 sequence detector (Applied Biosystems, Waltham, MA). Individual 50- $\mu$ l reaction mixtures containing TaqMan Gene Expression Master Mix (Applied Biosystems, Waltham, MA) and the thermal cycler conditions recommended in the manufacturer’s instructions were used. All samples were analyzed in triplicate. No amplification was evident in any no-template control. The relative expression of each target gene was calculated via the  $\Delta\Delta$  Ct method as described in the manufacturer’s instructions (Applied Biosystems, Waltham, MA). Differences in gene expression between control and hypothermic myocardium were assessed via the Student’s t test; P values of 0.05 or lower were considered statistically significant. In addition, this experiment was checked according to the quantitative real-time PCR experiment (MIQE) guidelines (Supplement 2) [20].

### Immunohistochemistry

Specimens were fixed in 4% buffered formalin, embedded in paraffin, and sectioned at a thickness of 2.5  $\mu$ m. Each section was stained with hematoxylin and eosin (H&E). In order to analyze histological dynamics, immunohistochemistry was performed. No

commercially suitable antibodies were found for two upregulated genes (*Cyp26b1*, *Atf3*) or three downregulated genes (*Slc41a3*, *Slc46a2*, *Nr1d1*). Therefore, expression of granzyme A was examined using rabbit anti-granzyme A (Cloud-Clone, Houston, TX) as the primary antibodies. Antigen activation was performed with a microwave oven and antigen activating solution (Nichirei, Tokyo, Japan). Sections were incubated with primary antibodies diluted 1:25 for 12 h in a humid chamber at 4 °C. Thereafter, sections were incubated with peroxidase-conjugated secondary antibody according to the manufacturer’s instructions (Histofine MAX-PO (R), Nichirei, Tokyo, Japan). The chromogen used to visualize antibody signal was 3, 3-diamino-benzidine (Nichirei, Tokyo, Japan), and the specimens were counterstained with hematoxylin. Quantitative analysis was difficult in cardiac tissue; therefore, expression was assessed qualitatively via light microscope.

### Results

#### DNA microarrays

**Quality control:** With the quality control measures, data from 17870 of the 39485 microarray genes could be used for further analysis.

**Identification of significantly regulated genes:** We identified 3438 genes that exhibited hypothermia-induced differential expression in mouse myocardium; 1704 were upregulated, and 1734 were downregulated. Of the upregulated genes, 120 genes increased by > 1.5-fold and ≤ 2-fold, five by > 2-fold and ≤ 3-fold, and three by > 3-fold. Among the genes confirmed as upregulated, granzyme A was the most upregulated gene with a 3.26-fold increase. For the downregulated genes, expression in hypothermic myocardium was lower than in control myocardium by < 0.6-fold and ≥ 0.5-fold for 22 genes, by < 0.5-fold and ≥ 0.4-fold for seven genes, and by < 0.4-fold for one gene. Solute carrier family 41 member 3 was the most downregulated gene with a 0.463-fold reduction. Upregulated genes and downregulated genes were arranged in order (descending or ascending, respectively) with respect to fold-change; Table 1 lists the 50 upregulated genes with a change greater than 1.6-fold, and Table 2 lists the 30 downregulated genes with a change of 0.6-fold or lower.

#### Gene-set analysis:

**KEGG analysis:** Significant variations were found in 79 pathways, and the gene sets that were upregulated or downregulated are summarized in Tables 3 and 4 respectively. A total of 57 pathways were significantly upregulated, and 22 pathways were downregulated. Upregulation of the viral myocarditis pathway was evident. But, no pathway related to granzyme A and/or activating transcription factor 3 was identified as significantly altered in hypothermic myocardium.

#### Publicly available database analysis:

**Analysis with Biocarta pathway:** In connection with the six selected genes (*Gzma*, *Cyp26b1*, *Atf3*, *Slc41a3*, *Slc46a2* and *Nr1d1*), a granzyme A-mediated apoptosis pathway was retrieved for *Gzma*. This pathway was significantly upregulated (Figure 1 and Table 5).

**Analysis with GeneAssist:** In connection with the six selected genes, the following five pathways were found in this database: the granzyme, granzyme A, and IL 9 pathways for *Gzma* and the MAPK signaling and TNF signaling pathways for *Atf3*. Among these five pathways, the granzyme pathway, granzyme A pathway (for *Gzma*), and MAPK signaling (for *Atf3*) were significantly upregulated (Table 5).

**Analysis of gene function category:** To investigate the biological functions involving the differentially regulated genes, we performed Gene Ontology category analysis. The 10 categories most commonly associated with these differentially regulated (upregulated or downregulated) genes included biological process, molecular function, and cellular component. The most commonly represented categories among upregulated and downregulated genes were cellular process, binding, cell, and cell part (Supplements 3 and 4).

#### Validation of gene expression results by quantitative PCR

We used quantitative PCR to validate microarray findings for three upregulated and three downregulated genes (Figure 2). Quantitative PCR findings were consistent with DNA microarray findings except that fold differences detected by the two methods were not identical for each gene. Among the downregulated genes, *Slc41a3* was decreased to a greater extent than *Slc46a2* or *Nr1d1* was.

#### Immunohistochemical analyses

Myocardium remained stable based on H&E-stained specimens.

No infiltration of inflammatory cells was seen in hypothermic specimens. Based on the immunohistochemical analyses, granzyme A expression was not evident in any control myocardium specimen; in contrast, slight granzyme A expression was evident in cytoplasm of hypothermic cardiac myocytes. There was no granzyme A expression in endocardial, epicardial, or endothelial cells (Figure 3).

#### Discussion

In the present study, DNA microarray analyses were performed with control and hypothermic ventricular myocardium. A total of 3438 genes were found to be differentially expressed in hypothermic tissue; specifically, 1704 were upregulated, and 1734 were downregulated. Cardiac candidates for forensic biomarkers of hypothermia were *Gzma*, *Cyp26b1*, and *Atf3* among the upregulated genes (Table 1) and *Slc41a3*, *Slc46a2*, and *Nr1d1* among the downregulated genes (Table 2). Needless to say, the possibility exists that other currently unidentified factors that are differentially expressed may be useful for diagnosing hypothermia. To our knowledge, no previous studies of hypothermia have identified a connection between hypothermia and *Gzma*, *Cyp26b1*, *Atf3*, *Slc41a3*, *Slc46a2* or *Nr1d1* expression. The Gene Ontology analysis indicated that cellular process, binding, cell, and cell part were significantly highly represented categories. The gene-set analysis revealed that cell death pathways related to granzyme A were upregulated and that these pathways may be involved in the cardiac pathogenesis of hypothermia.

Multiple types of cell death have been described; these include apoptosis, autophagy, necrosis, senescence, and mitotic catastrophe [21]. Some genes identified here as differentially regulated in response to hypothermia are modulators of one or more cell-death pathways; for example, granzyme A was upregulated in this study, and this protein leads to cell death by mediating cleavage of DNA molecules in the nucleus and of molecules in the nuclear envelope or mitochondrial membranes [21,22]. In addition, granzyme A plays an important role in inflammation [21]. Extracellular matrix components such as vitronectin, fibronectin, fibrinogen, laminin, and proteoglycans can be cleaved by granzyme A and this degradation may facilitate movements of leukocytes [21,23]. Granzyme A can also induce secretion of cytokines [24-26]. Activating transcription factor 3 was also upregulated in the hypothermic myocardium, and it is known to affect genes involved in apoptosis [27].

Decreased cardiac output and fatal arrhythmias are observed during hypothermia [14,15]. Histological analyses reveal that hypothermia causes degenerative foci in myocardium [28]; these foci consist of myofibrosis, calcifications, hyperchromasia, contraction bands, waving, discoloration and fragmentation of the fibers, edema, hemorrhages [3,29], coagulation necrosis, extravasation of red cells [3], inflammatory reactions (including cellular infiltration), granulation, and scarring [28,30,31]. Fatty changes in myocardium are also observed [32]. These histological lesions could act as foci of ventricular fibrillation [31]. Putative causative mechanisms include myocardial ischemia [33] mediated by platelet thrombi [31], increased blood viscosity [29,34-36], insufficient coronary perfusion, and catecholamine mobilizations [29]. Interestingly, our current findings suggested a previously unidentified putative mechanism for these lesions; specifically, hypothermia may induce myocardial cell death via granzyme A and activating transcription factor 3, and

**Table 3:** Gene-set analysis of the myocardial transcriptome in response to hypothermia with gene sets arranged by decreasing Z-score.

KEGG map	Map name	Number of genes	p-value	Fold change average	Z score
mmu05330	Allograft rejection	29	0.00E+00	0.352	8.544
mmu05320	Autoimmune thyroid disease	30	0.00E+00	0.338	8.319
mmu05332	Graft-versus-host disease	30	8.88E-16	0.327	8.056
mmu04514	Cell adhesion molecules (CAMs)	94	9.10E-15	0.181	7.750
mmu04612	Antigen processing and presentation	59	1.18E-14	0.226	7.719
mmu04940	Type I diabetes mellitus	37	8.04E-14	0.274	7.470
mmu04650	Natural killer cell mediated cytotoxicity	112	5.60E-12	0.149	6.889
mmu05150	Staphylococcus aureus infection	29	1.55E-09	0.251	6.039
mmu04145	Phagosome	155	2.95E-09	0.111	5.935
mmu05322	Systemic lupus erythematosus	90	6.44E-09	0.141	5.805
mmu04672	Intestinal immune network for IgA production	27	1.93E-08	0.243	5.618
mmu05416	Viral myocarditis	85	2.63E-08	0.139	5.564
mmu05164	Influenza A	160	8.74E-08	0.100	5.351
mmu05168	Herpes simplex infection	183	1.17E-07	0.093	5.299
mmu05166	HTLV-I infection	273	1.30E-07	0.077	5.279
mmu05340	Primary immunodeficiency	25	2.54E-06	0.212	4.705
mmu05203	Viral carcinogenesis	218	6.44E-06	0.074	4.511
mmu04662	B cell receptor signaling pathway	92	7.80E-06	0.109	4.471
mmu04060	Cytokine-cytokine receptor interaction	145	1.08E-05	0.087	4.400
mmu04062	Chemokine signaling pathway	168	1.51E-05	0.080	4.327
mmu04380	Osteoclast differentiation	129	3.68E-05	0.087	4.126
mmu04810	Regulation of actin cytoskeleton	229	6.53E-05	0.065	3.993
mmu04670	Leukocyte transendothelial migration	105	1.33E-04	0.089	3.822
mmu05202	Transcriptional misregulation in cancer	160	2.94E-04	0.070	3.620
mmu05310	Asthma	8	3.07E-04	0.285	3.609
mmu04510	Focal adhesion	218	5.52E-04	0.059	3.454
mmu05140	Leishmania infection	63	7.12E-04	0.100	3.385
mmu04110	Cell cycle	123	9.65E-04	0.072	3.301
mmu05152	Tuberculosis	154	1.01E-03	0.065	3.286
mmu05034	Alcoholism	148	1.03E-03	0.066	3.283
mmu04640	Hematopoietic cell lineage	54	1.21E-03	0.103	3.236
mmu05200	Pathways in cancer	331	1.62E-03	0.045	3.152
mmu03030	DNA Replication	39	2.45E-03	0.113	3.030
mmu04666	Fc gamma R-mediated phagocytosis	112	2.68E-03	0.069	3.003
mmu05143	African trypanosomiasis	23	2.90E-03	0.143	2.978
mmu05222	Small cell lung cancer	90	4.90E-03	0.072	2.814
mmu05133	Pertussis	72	7.17E-03	0.077	2.689
mmu04540	Gap junction	88	7.90E-03	0.069	2.657
mmu04630	Jak-STAT signaling pathway	110	8.14E-03	0.063	2.646
mmu05169	Epstein-Barr virus infection	232	8.97E-03	0.045	2.613
mmu04512	ECM-receptor interaction	67	9.22E-03	0.077	2.604
mmu04623	Cytosolic DNA-sensing pathway	49	9.62E-03	0.088	2.589
mmu05323	Rheumatoid arthritis	59	2.32E-02	0.072	2.270



mmu05160	Hepatitis C	123	2.40E-02	0.052	2.258
mmu05033	Nicotine addiction	6	2.72E-02	0.204	2.209
mmu04210	Apoptosis	87	2.78E-02	0.059	2.200
mmu05144	Malaria	34	2.97E-02	0.089	2.174
mmu05215	Prostate cancer	105	3.36E-02	0.053	2.124
mmu05145	Toxoplasmosis	123	3.40E-02	0.049	2.120
mmu04973	Carbohydrate digestion and absorption	31	3.50E-02	0.090	2.108
mmu04620	Toll-like receptor signaling pathway	87	3.62E-02	0.056	2.095
mmu05032	Morphine addiction	71	3.66E-02	0.062	2.091
mmu05218	Melanoma	78	3.91E-02	0.058	2.063
mmu04740	Olfactory transduction	47	4.10E-02	0.072	2.043
mmu04064		96	4.23E-02	0.053	2.031
mmu00524	Butirosin and neomycin biosynthesis	5	4.29E-02	0.204	2.025
mmu05162	Measles	124	4.54E-02	0.047	2.001

**Table 4:** Gene-set analysis of the myocardial transcriptome in response to hypothermia with gene sets arranged by increasing Z-score.

KEGG map	Map name	Number of genes	p-value	Fold change average	Z score
mmu00650	Butanoate metabolism	25	1.28E-04	-0.159	-3.831
mmu00480	Glutathione metabolism	63	4.27E-04	-0.089	-3.523
mmu00072	Synthesis and degradation of ketone bodies	10	4.34E-04	-0.234	-3.519
mmu01100	Metabolic pathways	1105	5.73E-04	-0.015	-3.444
mmu01040	Biosynthesis of unsaturated fatty acids	21	6.10E-04	-0.155	-3.427
mmu00280	Valine, leucine and isoleucine degradation	49	8.49E-04	-0.096	-3.336
mmu00062	Fatty acid elongation in mitochondria	19	1.12E-03	-0.155	-3.259
mmu00970	Aminoacyl-tRNA biosynthesis	44	2.27E-03	-0.092	-3.053
mmu00380	Tryptophan metabolism	35	3.00E-03	-0.101	-2.968
mmu04710	Circadian rhythm - mammal	22	6.54E-03	-0.118	-2.719
mmu03450	Non-homologous end-joining	13	7.43E-03	-0.154	-2.677
mmu03008	Ribosome biogenesis in eukaryotes	91	7.84E-03	-0.053	-2.659
mmu04146	Peroxisome	84	1.68E-02	-0.049	-2.392
mmu00982	Drug metabolism - cytochrome P450	47	1.91E-02	-0.067	-2.345
mmu00071	Fatty acid metabolism	41	1.99E-02	-0.071	-2.328
mmu00670	One carbon pool by folate	19	2.59E-02	-0.103	-2.227
mmu03010	Ribosome	194	2.91E-02	-0.026	-2.183
mmu00640	Propanoate metabolism	35	3.04E-02	-0.072	-2.165
mmu00450	Selenoamino acid metabolism	17	3.19E-02	-0.105	-2.146
mmu00591	Linoleic acid metabolism	16	3.29E-02	-0.108	-2.134
mmu04950	Maturity onset diabetes of the young	9	4.64E-02	-0.136	-1.991
mmu04721	Synaptic vesicle cycle	54	4.87E-02	-0.051	-1.971

this cell death may cause some of the histological lesions and clinical symptoms characteristic of hypothermic myocardium. Some clinical studies show that hypothermia causes high mortality [13]. Myocardial cell deaths induced by hypothermia would be irreversible changes, and we postulate that this cell death may be related to the circulatory failure, resistance to treatment, and high mortality associated with hypothermia.

A compact arrangement of myocardial fibers (called interstitial narrowness) between myocardial fibers has recently been identified as a histological finding indicative of hypothermia [37]. Some pathologists have proposed that this finding is caused by dehydration during hypothermia [38]. The present transcriptome analysis did not provide substantial insight into this mechanism and related genetic pathways responsible for this phenomenon. One might say

**Table 5:** Gene-set analyses of the myocardium transcriptome in response to hypothermia based on publicly available pathway databases.

Map name	Number of genes	p-value	Fold change average	Z score
<b>A. Biocarta pathway</b>				
a) Granzyme A				
Granzyme A mediated apoptosis pathway	16	1.43E-02	0.141	2.449
<b>B. Geneassist</b>				
a) Granzyme A				
Granzyme A pathway	15	1.53E-02	0.144	2.426
Granzyme pathway	40	2.48E-02	0.085	2.245
IL-9pathway	37	0.707148067	-0.006	-0.376
b) Activating transcription factor 3				
MAPK Signaling	455	8.71E-03	0.034	2.623
TNF Signaling	72	0.06963688	0.054	1.814

that interstitial narrowness is a passive myocardial change caused by dehydration.

The present research demonstrated changes in gene expression in hypothermic murine myocardium and identified potential cardiac candidates for forensic biomarkers of hypothermia. The present findings suggested that myocardial cell death was induced in hypothermia and that this cell death could cause cardiac dysfunctions and high mortality during hypothermia. These data may help elucidate the pathophysiology of hypothermia. But mechanisms of hypothermia may be multifactorial and manifold. In addition, reports of forensic hypothermia investigations that use molecular biological techniques have only recently begun to appear, and traditional characteristics of hypothermia remain important for forensic diagnosis [39]. Large-scale gene analyses, including DNA microarray analyses, are promising methods for detecting forensic pathological biomarkers. However, it should be noted that applications of these gene expression data would be limited in routine forensic practices. For example, the postmortem interval could negatively affect gene expression analysis. The samples in these animal experiments were collected under ideal circumstances. After considering these transcriptomic data along with postmortem changes, expression of biomarker candidates in forensic human samples should be assessed. Because RNA decomposes in the postmortem interval, utilization of protein markers should be considered as alternative to RNA biomarkers. Therefore, analysis of the proteins encoded by candidate biomarkers identified via this DNA microarray analysis is a next step in the process of identifying clinically useful biomarkers. The present histological study also demonstrated slight expression of granzyme A in cardiac myocytes. Importantly, results of the present murine DNA microarray study may provide data applicable to the development of future immunohistochemical protocols for analysis of human forensic samples. In addition, we believe that these data are informative, not only for future forensic pathological studies, but also potentially for clinical research into hypothermia.

**Conclusion**

We compared the hypothermic murine myocardial transcriptome to that of a room-temperature control using DNA microarray technology; we thereby identified 3438 genes that were

significantly differentially expressed in response to hypothermia. Of these genes, 1704 were upregulated and 1734 were downregulated. The gene encoding granzyme A was the most upregulated gene, and that encoding solute carrier family 41 member 3 was the most downregulated. In our gene-set analysis, significant variations were found in 79 pathways, and we suggest that pathways related to granzyme A and cell death may be involved in hypothermia-induced cardiac pathogenesis. The present study documented acute myocardial responses during hypothermia and revealed cardiac candidates that may be useful as forensic biomarkers of hypothermia. Myocardial cell death induced by granzyme A may represent an irreversible change that is related to the circulatory failure, resistance to treatment, and high mortality associated with hypothermia. Furthermore, the present microarray data may facilitate development of protocols for immunohistochemical analysis of specimens from human cases and be beneficial to clinical research on hypothermia.

**References**

- Ulrich AS, Rathlev NK (2004) Hypothermia and localized cold injuries. *Emerg Med Clin North Am* 22: 281-298.
- Saukko P, Knight B (2004) Neglect, starvation and hypothermia: Injury caused by cold: hypothermia. In: Saukko P, Knight B, (Eds) *Knight's Forensic Pathology* (3<sup>rd</sup> Edn), Edward Arnold (Publishers) Ltd, CRC Press, London, pp. 414-420.
- Hirvonen J (1976) Necropsy findings in fatal hypothermia cases. *Forensic Sci* 8: 155-164.
- Aghayev E, Thali MJ, Jackowski C, Sonnenschein M, Dirnhofer R, et al. (2008) MRI detects hemorrhages in the muscles of the back in hypothermia. *Forensic Sci Int* 176: 183-186.
- Paton BC (1983) Accidental hypothermia. *Pharmacol Ther* 22: 331-377.
- DiMaio VJ, DiMaio D (2001) Hyperthermia and Hypothermia: The effects of heat and cold. In: DiMaio VJ, DiMaio D, (Eds) *Forensic pathology* (2<sup>nd</sup> Edn), CRC press, Boca Raton, pp. 419-434.
- Fisher ER, Fedor EJ, Fisher B (1957) Pathologic and histochemical observations in experimental hypothermia. *AMA Arch Surg* 75: 817-827.
- Mant AK (1969) Autopsy diagnosis of accidental hypothermia. *J Forensic Med* 16: 126-129.
- Preuss J, Dettmeyer R, Lignitz E, Madea B (2004) Fatty degeneration in renal tubule epithelium in accidental hypothermia victims. *Forensic Sci Int* 141: 131-135.

10. Preuss J, Lignitz E, Dettmeyer R, Madea B (2007) Pancreatic changes in cases of death due to hypothermia. *Forensic Sci Int* 166: 194-198.
11. Preuss J, Dettmeyer R, Poster S, Lignitz E, Madea B (2008) The expression of heat shock protein 70 in kidneys in cases of death due to hypothermia. *Forensic Sci Int* 176: 248-252.
12. Hirvonen J, Huttunen P (1982) Increased urinary concentration of catecholamines in hypothermia deaths. *J Forensic Sci* 27: 264-271.
13. Vassal T, Benoit-Gonin B, Carrat F, Guidet B, Maury E, et al. (2001) Severe accidental hypothermia treated in an ICU: prognosis and outcome. *Chest* 120: 1998-2003.
14. Lauri T, Leskinen M, Timisjarvi J, Hirvonen L (1991) Cardiac function in hypothermia. *Arctic Med Res* 50 Suppl 6: 63-66.
15. Maaravi Y, Weiss AT (1990) The effect of prolonged hypothermia on cardiac function in a young patient with accidental hypothermia. *Chest* 98: 1019-1020.
16. Okuda C, Saito A, Miyazaki M, Kuriyama K (1986) Alteration of the turnover of dopamine and 5-hydroxytryptamine in rat brain associated with hypothermia. *Pharmacol Biochem Behav* 24: 79-83.
17. Brazma A, Hingamp P, Quackenbush J, Sherlock G, Spellman P, et al. (2001) Minimum information about a microarray experiment (MIAME)-toward standards for microarray data. *Nat Genet* 29: 365-371.
18. Kim SY, Volsky DJ (2005) PAGE: Parametric analysis of gene set enrichment. *BMC Bioinformatics* 6: 144.
19. Vandesompele J, De Preter K, Pattyn F, Poppe B, Van Roy N, et al. (2002) Accurate normalization of real-time quantitative RT-PCR data by geometric averaging of multiple internal control genes. *Genome Biol* 3: RESEARCH0034.
20. Bustin SA, Benes V, Garson JA, Hellemans J, Huggett J, et al. (2009) The MIQE guidelines: minimum information for publication of quantitative real-time PCR experiments. *Clin Chem* 55: 611-622.
21. Zhou F (2010) Expression of multiple granzymes by cytotoxic T lymphocyte implies that they activate diverse apoptotic pathways in target cells. *Int Rev Immunol* 29: 38-55.
22. Susanto O, Trapani JA, Brasacchio D (2012) Controversies in granzyme biology. *Tissue Antigens* 80: 477-487.
23. Buzza MS, Bird PI (2006) Extracellular granzymes: current perspectives. *Biol Chem* 387: 827-837.
24. Metkar SS, Mena C, Pardo J, Wang B, Wallich R, et al. (2008) Human and mouse granzyme A induce a proinflammatory cytokine response. *Immunity* 29: 720-733.
25. Sower LE, Klimpel GR, Hanna W, Froelich CJ (1996) Extracellular activities of human granzymes. I. Granzyme A induces IL6 and IL8 production in fibroblast and epithelial cell lines. *Cell Immunol* 171: 159-163.
26. Yoshikawa Y, Hirayasu H, Tsuzuki S, Fushiki T (2008) Granzyme A causes detachment of alveolar epithelial A549 cells accompanied by promotion of interleukin-8 release. *Biosci Biotechnol Biochem* 72: 2481-2484.
27. Turchi L, Aberdam E, Mazure N, Pouyssegur J, Deckert M, et al. (2008) Hif-2alpha mediates UV-induced apoptosis through a novel ATF3-dependent death pathway. *Cell Death Differ* 15: 1472-1480.
28. Hirvonen J, Huttunen P, Hiltunen K (1988) Creatine phosphokinase in serum and cerebrospinal fluid, and microscopic findings in brain and heart in hypothermic rabbits. *Forensic Sci Int* 39: 271-278.
29. Hirvonen J, Penttinen J, Huttunen P, Saukko P (1980) Changes in the myocardium and skeletal muscle in guinea pigs in cold exposure with and without ethanol. *Z Rechtsmed* 84: 195-207.
30. Altland PD, Highman B, Sellner RG (1974) Serum enzyme and tissue changes in shaven rabbits exposed to cold. *Cryobiology* 11: 296-304.
31. Sarajas HS (1964) Myocardial damage induced by immersion hypothermia. *Am J Cardiol* 13: 355-366.
32. Preuss J, Dettmeyer R, Lignitz E, Madea B (2006) Fatty degeneration of myocardial cells as a sign of death due to hypothermia versus degenerative deposition of lipofuscin. *Forensic Sci Int* 159: 1-5.
33. Lynch HF, Adolph EF (1957) Blood flow in small blood vessels during deep hypothermia. *J Appl Physiol* 11: 192-196.
34. Kanter GS (1968) Hypothermic hemoconcentration. *Am J Physiol* 214: 856-859.
35. Keen G, Gerbode F (1963) Observations on the microcirculation during profound hypothermia. *J Thorac Cardiovasc Surg* 45: 252-260.
36. Taylor MJ, Bailes JE, Elrifai AM, Shih SR, Teeple E, et al. (1995) A new solution for life without blood. Asanguineous low-flow perfusion of a whole-body perfusate during 3 hours of cardiac arrest and profound hypothermia. *Circulation* 91: 431-444.
37. Funayama M, Morita M, Shimizu K, Shiono H, Hiraiwa K, et al. (1997) Compact arrangement of myocardial fibers in cases of fatal hypothermia. Proceeding of 14th meeting of International Association of Forensic Sciences. *Curr Top Forensic Sci* 3: 381-383.
38. Jolly BT, Ghezzi KT (1992) Accidental hypothermia. *Emerg Med Clin North Am* 10: 311-327.
39. Turk EE (2010) Hypothermia. *Forensic Sci Med Pathol* 6: 106-115.

## Acknowledgements

This study was supported by JSPS KAKENHI grant number 26460884.